The Journal of Neuroscience, August 1, 1996, *16*(15):4543–4550

Phenotypic Alteration of a Human BK (*hSlo*) Channel by *hSloβ* Subunit Coexpression: Changes in Blocker Sensitivity, Activation/ Relaxation and Inactivation Kinetics, and Protein Kinase A Modulation

Steven I. Dworetzky, Christopher G. Boissard, Janet T. Lum-Ragan, M. Craig McKay, Debra J. Post-Munson, Joanne T. Trojnacki, Chia-Ping Chang, and Valentin K. Gribkoff

Central Nervous System Drug Discovery, Bristol-Myers Squibb Pharmaceutical Research Institute, Wallingford, Connecticut 06492

A human homolog of the large-conductance calcium-activated potassium (BK) channel β subunit (*hSloβ*) was cloned, and its effects on a human BK channel (*hSlo*) phenotype are reported. Coexpression of *hSlo* and *hSloβ*, in both oocytes and human embryonic kidney 293 cells, resulted in increased Ca^{2+} sensitivity, marked slowing of BK channel activation and relaxation, and a significant reduction in slow inactivation. In addition, coexpression changed the pharmacology of the BK channel phenotype: *hSlo*-mediated currents in oocytes were more sensitive to the peptide toxin iberiotoxin than were *hSlo* + *hSloβ* currents, and the potency of blockade by the alkaloid BK blocker tetrandrine was much greater on *hSlo* + *hSloβ*-mediated currents compared with *hSlo* currents alone. No significant differences in the response to charybdotoxin or the BK channel opener NS1619 were observed. Modulation of BK channel activity by phosphorylation was also affected by the presence of the *hSloβ* subunit. Application of cAMP-dependent protein kinase increased P_{OPEN} of *hSlo* channels, but decreased P_{OPEN} of most *hSlo* + *hSloβ* channels. Taken together, these altered characteristics may explain some of the wide diversity of BK channel phenotypes observed in native tissues.

Key words: BK channels; coexpression; hSlo*; modulation; channel blockers; BK phenotypes*

Potassium channels are the most diverse class of ion channels. The voltage-dependent potassium (K^+) channels achieve phenotypic variation in part through the evolution of gene families coding for similar channels (Pongs, 1992; Salkoff et al., 1992; Chandy and Gutman, 1995), unlike another important class of K^+ channels, the large-conductance calcium (Ca^{2+})-activated K^+ (BK) channels (Robitaille and Charlton, 1992; Bielefeldt and Jackson, 1993). BK channels are regulated by both voltage and internal calcium concentration; these factors, together with their large single-channel conductance, make them very effective regulators of cell excitability, particularly adapted to monitoring and indirectly regulating calcium entry. BK channels have multiple phenotypes (Latorre et al., 1989; Reinhart et al., 1989; Wang and Lemos, 1992), but, to date, only one gene has been identified (Atkinson et al., 1991; Adelman et al., 1992; Butler et al., 1993; Dworetzky et al., 1994; Pallanck and Ganetzky, 1994). At least two phenotypes exist in rat brain: type I BK channels (fast-gating, BK toxin-sensitive channels activated by cAMP-dependent protein phosphorylation) and type II BK channels (relatively toxin-insensitive, slowly-gating, blocked by the alkaloid tetrandrine, with activity reduced by cAMP-dependent protein phosphorylation) (Reinhart et al., 1989, 1991; Wang and Lemos, 1992). Alternative exon splice variation confers different properties on BK channels, particularly in relation to calcium sensitivity, but this does not seem to be sufficient to account for these major phenotypic classes (Lagrutta et al., 1994; Tseng-Crank et al., 1994). Regulatory (β) subunits have been shown to alter rates of inactivation of voltage-dependent K^+ channels (Rettig et al., 1994), and a recently cloned bovine BK channel β subunit (Knaus et al., 1994) was found to increase the sensitivity of cloned BK channels to Ca^{2+} (McCobb et al., 1995; McManus et al., 1995) and to the BK channel opener DHS-1 (McManus et al., 1995). In this study, we report the cloning of a human BK β subunit (*hSloβ*) and describe how coexpression alters the biophysical and pharmacological characteristics of a cloned human BK channel.

Received March 7, 1996; revised May 3, 1996; accepted May 7, 1996.

Correspondence should be addressed to Dr. Valentin K. Gribkoff, Central Nervous System Drug Discovery, Department 404, Bristol-Myers Squibb Pharmaceutical Research Institute, 5 Research Parkway, Wallingford, CT 06492.

MATERIALS AND METHODS

Cloning of the human β subunit. PCR primers were designed adjacent to the 5′ and 3′ end of the bovine β subunit sequence (Knaus et al., 1994) and used to amplify partial clones by PCR (45 sec, 94°C; 60 sec, 45°C; 75 sec, 72°C; 35 cycles) from reverse-transcribed human tracheal poly A^+ RNA. The resulting DNA fragment was isolated, purified, random-prime-labeled with deoxycytidine [α-^{32}P]triphosphate, and used to screen a human uterus cDNA library (Clontech, Palo Alto, CA). The filters were hybridized in 30% formamide, 2X PIPES, and 1% SDS at 42°C, and washed in 0.1× SSC, 0.1% SDS at 42°C. Resulting positive plaques were plate-purified, and the inserts were isolated by *Eco*RI restriction enzyme digestion. Positive clonal inserts were ligated into pBluescriptKS$^+$ (Stratagene, La Jolla, CA), and both strands were sequenced by dideoxy termination reactions. To remove the 5′ and 3′ untranslated regions of the *hSloβ* clone, synthetic oligonucleotide primers were designed to amplify only the *hSloβ* coding region with a T3 RNA polymerase and Kozak consensus sequence (Kozak, 1987) added to the 5′ end [forward primer; 5′-CGCAATTAACCCTCACTAAAGGGCGCCACCATGGTGAAGAAGCTGGTGATGGCC-3′ and reverse primer; 5′-GCATGGATGGATGTCACTACTTCTGG-3′]. The *hSloβ* PCR product was subcloned into the pCRII TA cloning vector (Invitrogen, San Diego, CA), sequenced to verify possible PCR amplification errors, and used for preparation of cRNA. The original *hSloβ* insert was also subcloned into

Table 1. Activation and relaxation kinetics of *hSlo* and *hSlo + hSloβ*

Expressed channel	Activation (outside-out patch)	Relaxation (inside-out patch)	Time to peak current (outside-out patch)	Time to peak current (two-electrode voltage clamp, oocytes)
hSlo	τ_1 = 1.17 msec ± 0.25	τ_1 = 2.57 msec ± 0.39	28.7 msec ± 5.8	11.76 msec ± 0.86
	τ_2 = 10.78 msec ± 3.02	τ_2 = 15.78 msec ± 4.35		
	$n = 7$	$n = 5$	$n = 7$	$n = 5$
hSlo + hSloβ	τ_1 = 9.27 msec ± 0.83**	τ_1 = 4.01 msec ± 0.50*	145.6 msec ± 19.6*	24.24 msec ± 1.55**
	τ_2 = 48.89 msec ± 12.10**	τ_2 = 28.37 msec ± 9.14		
	$n = 4$	$n = 4$	$n = 6$	$n = 5$

Several methods were used to examine the relative activation rates of *hSlo* and *hSlo + hSloβ* BK channels in HEK 293 cells and oocytes. Current activation and relaxation kinetics were best fit using a two-component exponential model of the form $y = A1 \times \exp[-(t - t_o)/\tau_1] + A2 \times \exp[-(t - t_o)/\tau_2] + C$ (see text). Time to peak currents were directly measured. Values given for oocyte times to peak current are for a voltage step between −60 and 140 mV; details of all other recordings are given in the description of experimental procedures. All values are mean ± SEM. Comparisons are two-tailed *t* tests. *hSlo + hSloβ versus hSlo*, $^*p < 0.05$, $^{**}p < 0.005$.

pcDNA3 (Invitrogen) for mammalian expression in human embryonic kidney (HEK) 293 cells. The *hSloβ* clone was tested for expression by *in vitro* transcription and translation (not shown). The Genbank accession number for the *hSloβ* clone is U38907.

Expression and recording in Xenopus *oocytes.* The *hSlo* and *hSloβ* cDNAs were linearized with the restriction enzyme *Not*I and *Bam*HI, respectively, and *in vitro* transcribed using the mMessage mMachine T3 RNA polymerase kit according to the manufacturer's instructions (Ambion, Austin, TX). The cRNAs were solubilized in RNase-free water and stored at −70°C at a concentration of 1.5 μg/μl. The *hSlo* construct used in the present experiments was originally cloned from a human brain substantia nigra cDNA library (Dworetzky et al., 1994) and did not contain any of the previously identified alternative splice exons (Dworetzky et al., 1994; Tseng-Crank et al., 1994). Frog oocytes were prepared and injected using standard techniques (Colman, 1984). In *hSlo + hSloβ* coexpression experiments, each oocyte was injected with ~50 nl of the appropriate cRNA, resulting in total injections of 100 nl/oocyte. Injection of equivalent amounts of *hSlo* cRNA (50 nl) supplemented with 50 nl of RNase-free water did not alter the characteristics of *hSlo* currents. After injection, oocytes were maintained at 17°C in ND96 medium consisting of (in mM): 90 NaCl, 1.0 KCl, 1.0 $CaCl_2$, 1.0 $MgCl_2$, 5.0 HEPES, pH 7.5. Horse serum and penicillin/streptomycin, both 5% of final volume, were added as supplements to the incubation medium. Electrophysiological recording commenced 2–6 d after cRNA injection. Before the start of an experiment, oocytes were placed in a recording chamber and incubated in modified Barth's solution (MBS) consisting of (in mM): 88 NaCl, 2.4 $NaHCO_3$, 1.0 KCl, 10 HEPES, 0.82 $MgSO_4$, 0.33 $Ca(NO_3)_2$, 0.41 $CaCl_2$, pH 7.5. Oocytes were impaled with electrodes (1–2 MΩ), and standard, two-electrode voltage-clamp techniques were used to record whole-cell membrane currents (Stuhmer, 1992; GeneClamp 500, Axon Instruments, or Turbo TEC01C, Adams and List). Voltage-clamp protocols typically consisted of a series of voltage steps 100–750 msec duration in 20 mV steps from a holding potential of −60 mV to a maximal potential of 100–140 mV; records were digitized at 5 kHz and stored on a computer with pClamp 6.0 or AxoData software (Axon Instruments, Foster City, CA).

Expression and recording in HEK 293 cells. HEK 293 cells were plated on poly-D-lysine-coated coverslips at 10–20% confluency and transiently transfected 3 d later with either *hSlo* (1 μg DNA/35 mm dish) or *hSlo + hSloβ* (0.75 μg of each DNA/35 mm dish) by the lipofectamine method according to the manufacturer's instructions (Life Technologies, Gaithersburg, MD). Whole-cell and excised patch voltage-clamp recordings were made with standard techniques (Hamill et al., 1981) 24–72 hr after transfection. An Axopatch 200 amplifier and pClamp 6.0 software (Axon Instruments) were used for all recordings. The bath solution for both whole-cell and outside-out patch recordings contained (in mM): 145 NaCl, 3 KCl, 2.5 $CaCl_2$, 1 $MgCl_2$, 10 HEPES, pH 7.4. The internal solution for whole-cell recordings was (in mM): 140 KCl, 20 MOPS, 0.2 K_2EGTA, 0.174 $CaCl_2$ (1 μM estimated $[Ca^{2+}]_{free}$), pH 7.2. The pipette-filling solution and the bath solution used for inside-out excised patch recordings contained (in mM): 140 KCl, 20 MOPS, 1 K_2EGTA, pH 7.2. $CaCl_2$ was added to adjust free $[Ca^{2+}]$. Pipettes (2.5–5.0 MΩ in bath solution) were pulled from borosilicate glass, coated with SYLGARD, and fire-polished. Whole-cell currents were evoked by step depolarization of the membrane potential from −60 to 100 mV in 20 mV increments. Leakage currents, which were negligible, were uncorrected, and series resistance was compensated ~80%. Data were filtered at 2 or 5 kHz and digitized at 10 or 40 kHz. Ensemble averages of excised patch records were made by repetitively stepping (50–200 sweeps) the membrane potential of outside-out patches from −60 to 40 mV every 2 sec. Capacitance and leak compensation were made with amplifier controls. Records were filtered at 1–2 kHz and digitized at 10 kHz. The control free $[Ca^{2+}]$ was determined to be 0.79 μM; this and all free $[Ca^{2+}]$ were determined by a Fura-2 fluorometric assay in accord with the manufacturer's instructions (Molecular Probes, Eugene, OR). Average ensemble and whole-cell currents were best fit by a least-squares minimized, two-component exponential function of the form $y = A1 \times \exp[-(t - t_0)/\tau_1] + A2 \times \exp[-(t - t_0)/\tau_2] + C$, where A is the current amplitude, τ is the time constant, and C is the asymptotic current value. In most cases, two-tailed *t* tests were used to determine statistical significance of the differences in time-to-peak, τ_1, and τ_2 values.

Blocker and opener pharmacology. All drug solutions were introduced into the bath by gravity flow. Iberiotoxin (IbTX) and charybdotoxin (ChTX) (Peptides International, Louisville, KY) were prepared as aqueous stocks and diluted in MBS before use; tetrandrine (Aldrich, Milwaukee, WI) was prepared as a stock solution in dimethylformamide or dimethylsulfoxide (DMSO) and likewise diluted in the appropriate solution just before use. For IbTX and ChTX experiments, maximal suppression was defined as the peak suppression observed in response to 100–250 nM IbTX or 250–500 nM ChTX. These concentrations were sufficient to block all of the expressed current. Blockers were applied for at least 10 min. Logistic fits of the concentration–response relationships and EC_{50} estimates were obtained with KaleidoGraph software (Abelbeck). The BK channel opener NS1619 (Olesen et al., 1994) was made in-house, dissolved in DMSO (20 mM stock), and diluted to final concentration just before use.

Protein kinase A modulation. The effects of exposure to the catalytic subunit of the cAMP-dependent protein kinase A (PKA) (Promega, Madison, WI) on inside-out patches containing either *hSlo* or *hSlo + hSloβ* bathed with symmetrical 140 mM KCl solutions were measured by continuously monitoring steady-state changes in NP_{open} ($NP_{open} = I/i$; n = number of active channels; P_{open} is the open probability, I is the mean current, and i is the single-channel current amplitude; bin width 5 sec) before and during application of 60 nM PKA in the bath solution. The bath solution also contained 500 μM Mg^{2+}-ATP throughout the experiment. The free $[Ca^{2+}]$ of the bathing solution was 4.52 μM. Holding voltage was adjusted so that some channel closures to baseline were observed in the control solution. Recordings were filtered at 1 kHz and digitized at 10 kHz.

RESULTS

β subunit cloning

hSloβ was cloned by reverse transcription of human tracheal tissue and amplification of the cDNA via PCR protocols; the design of the oligonucleotide primers was based on the reported bovine sequence (Knaus et al., 1994). The amplified human DNA fragment was then used as a probe to screen a human uterus cDNA library. This library was used because of the low abundance of β subunit message present in brain (our unpublished results).

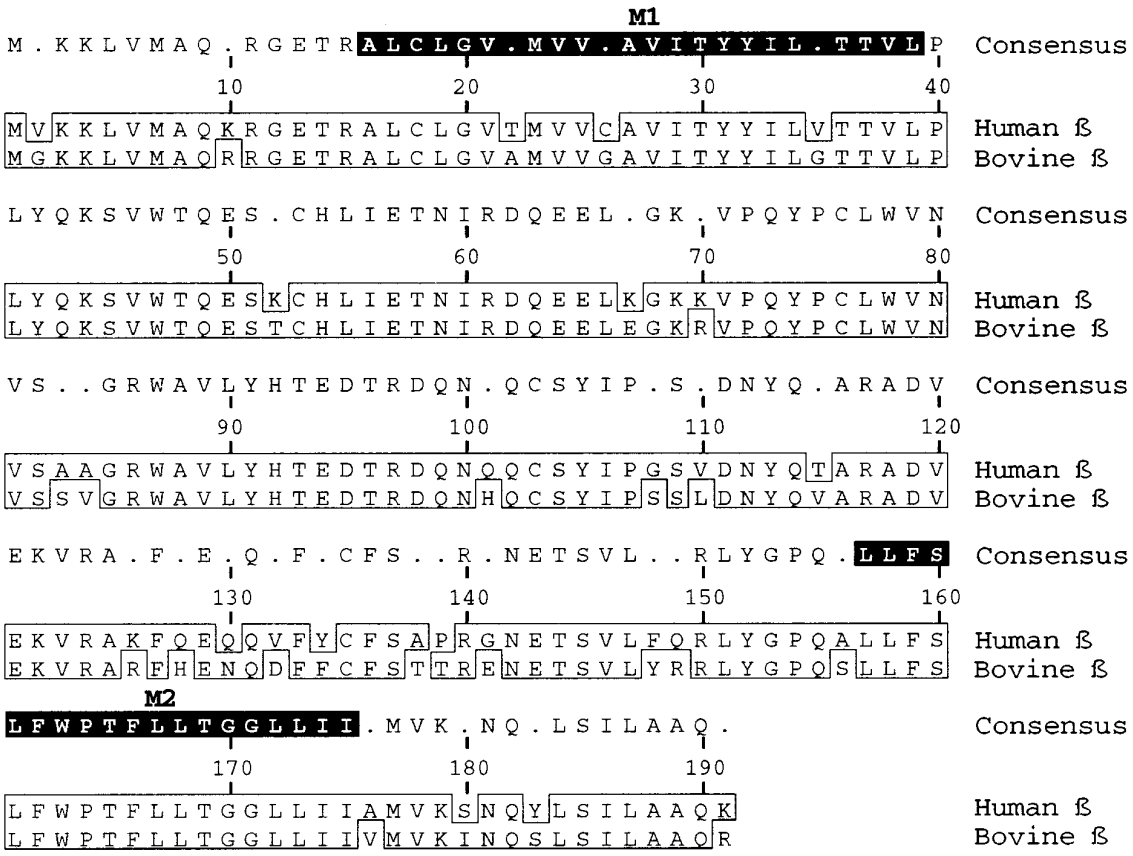

Figure 1. Predicted primary sequence of a cloned human BK channel β subunit (*hSlo*β) and its alignment with a bovine β subunit. The identical amino acids are *boxed* together, resulting in 85% identity between these sequences with the putative *M2* transmembrane domain being completely conserved. The putative transmembrane domains *M1* and *M2* are marked within the consensus sequence by the *black boxes*.

Numerous positive plaques were identified, and of the four clones carried through plaque isolation, all proved to be β subunit homologs with various amounts of 5′ and 3′ untranslated sequence. Alignment of the human and bovine protein sequences shows 85% identity (Fig. 1). The rat brain and smooth muscle β subunit sequences, which are highly homologous to the human and bovine sequences, were identical to each other (our unpublished results), and there is unlikely to be any difference between the human smooth muscle and human brain β subunit.

Activation/relaxation and inactivation kinetics

In general, *hSlo* produced rapidly activating currents in response to depolarization, and partial slow inactivation was observed with long voltage pulses. Coexpression of *hSlo* and the *hSlo*β subunit produced more slowly activating currents in which slow inactivation was greatly reduced (see below). Coexpression of *hSlo*β with the voltage-dependent K^+ channels $K_V1.3$, $K_V1.4$, and $K_V1.5$ produced no detectable difference in activation, inactivation, or peak amplitude values of currents mediated by these channels (data not shown). Oocytes injected with *hSlo*β alone did not produce any detectable current, and there was no noticeable alteration in the characteristics of the native oocyte current.

Although steady-state channel kinetics could not be studied because of the large number of channels in most excised patches, we could directly measure the activation kinetics of *hSlo* and *hSlo* + *hSlo*β. Excised and whole-cell patch-clamp recordings from transiently transfected HEK 293 cells and two-electrode voltage-clamp recordings in oocytes demonstrated that activation of *hSlo* channels was fast, whereas activation of *hSlo* + *hSlo*β channels was significantly slower (Fig. 2, Table 1; all values are mean ± SEM throughout). Current relaxation was similarly influenced by *hSlo*β coexpression (Table 1). The difference in activation kinetics was maintained when examined at multiple voltage-step values (−60 mV to 60, 80, and 100 mV, whole-cell patch recording in HEK 293 cells). At 60, 80, and 100 mV, respectively ($n = 5$), *hSlo* current activation time constants were $\tau_1 = 1.57 \pm 0.20$ msec, 1.25 ± 0.18 msec, and 0.89 ± 0.10 msec, and $\tau_2 = 20.96 \pm 5.59$ msec, 16.13 ± 7.63 msec, and 10.22 ± 4.87 msec, whereas corresponding values for *hSlo* + *hSlo*β ($n = 5$) were $\tau_1 = 10.22 \pm 2.74$ msec, 9.98 ± 2.12 msec, and 6.64 ± 1.39 msec, and $\tau_2 = 77.49 \pm 24.20$ msec, 84.91 ± 28.40 msec, and 56.10 ± 28.18 msec (repeated measures ANOVA; τ_1: $F = 10.61$, $p < 0.0001$; τ_2: $F = 3.69$, $p = 0.016$). In oocytes, a similar difference between the experimental groups was observed when time to peak current was measured at voltage steps from −60 mV (hold) to 60–140 mV in 20 mV increments (data for steps to 140 mV shown in Table 1; $F = 72.4$, $p < 0.0001$). Slow current inactivation was significantly reduced and slowed in oocytes and HEK 293 cells expressing *hSlo* + *hS3lo*β (Figs. 2, 3), and *hSlo* currents in oocytes recovered from inactivation significantly more slowly (Fig. 3).

As reported previously, coexpression of *mSlo* and *bSlo*β (bovine) resulted in a significant increase in the Ca^{2+} sensitivity of the expressed BK channels (McCobb et al., 1995; McManus et al., 1995). Similar results were obtained with *hSlo* and *hSlo*β coexpression. This was observed as a leftward shift in the conductance/

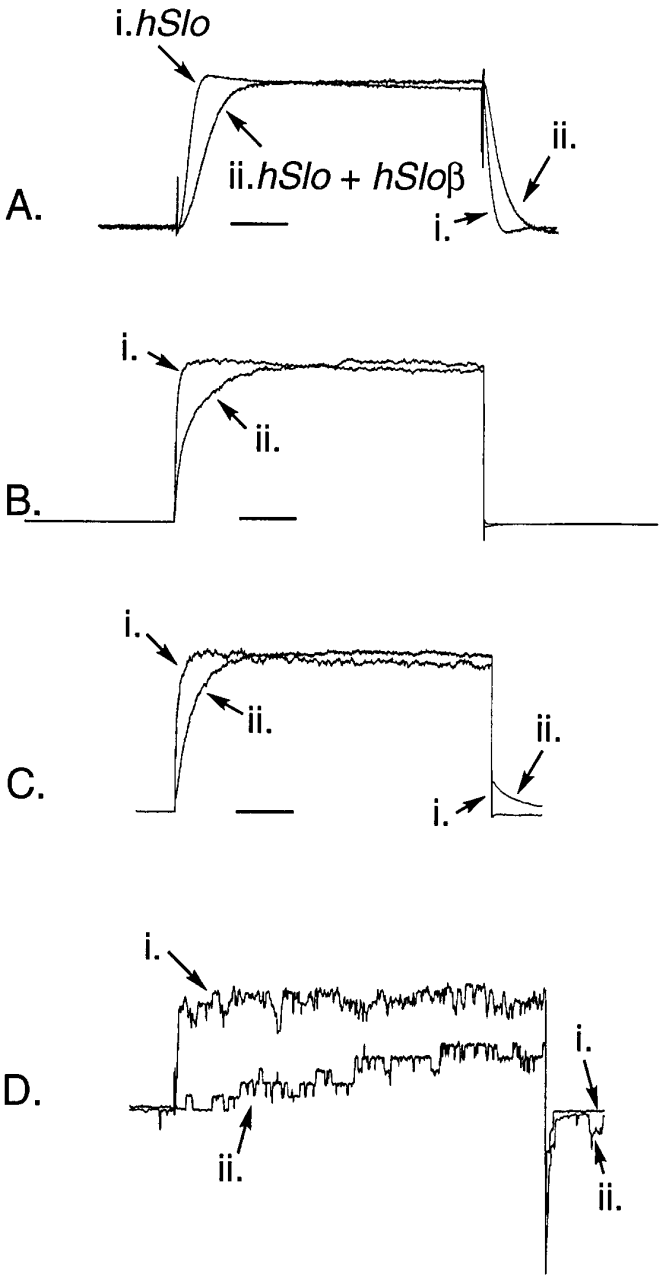

Figure 2. Activation records for *hSlo* and *hSlo* + *hSloβ* BK channels in oocytes and HEK 293 cells. Activation of *hSlo* + *hSloβ* BK currents was significantly slower than currents mediated by *hSlo* expression in *Xenopus* oocytes (*A*) and HEK 293 cells (*B*; whole-cell patch recordings, *C*; ensemble average currents from excised membrane patches, *D*; excised patch recordings, *single traces*). Currents were normalized for presentation. Peak current values in *A*, 6.4 μA for *hSlo* and 4.6 μA for *hSlo* + *hSloβ*; currents shown are in response to a depolarizing step from −60 to 80 mV. In *B*, 17.1 nA for *hSlo* and 11.7 nA for *hSlo* + *hSloβ*; currents shown resulted from voltage steps from −60 to 100 mV. In *C*, 114 pA for *hSlo* and 355 pA for *hSlo* + *hSloβ*. Horizontal axis scale: 20 msec for *A* and *B*, 40 msec for *C*. The currents in *C* and *D* resulted from voltage steps from −60 to 40 mV. The pulse duration for the multichannel recordings in *D* is 200 msec; note that the patches contain different (and large) numbers of channels; initial amplitude (*i.*) is 110 pA. No significant difference was observed in the amplitudes of *hSlo* or *hSlo* + *hSloβ* currents in either expression system after comparable incubation periods; likewise, no difference was observed in the single-channel slope conductance of channels coded by these constructs when currents from patches with a small number of channels were recorded (*hSlo* = 286 ± 12 pS, $n = 5$; *hSlo* + *hSloβ* = 289 ± 6 pS, $n = 4$). Note that deactivation of *hSlo* + *hSloβ* currents was also slower, as indicated in *A* and visible in *C* and *D* (see Table 1).

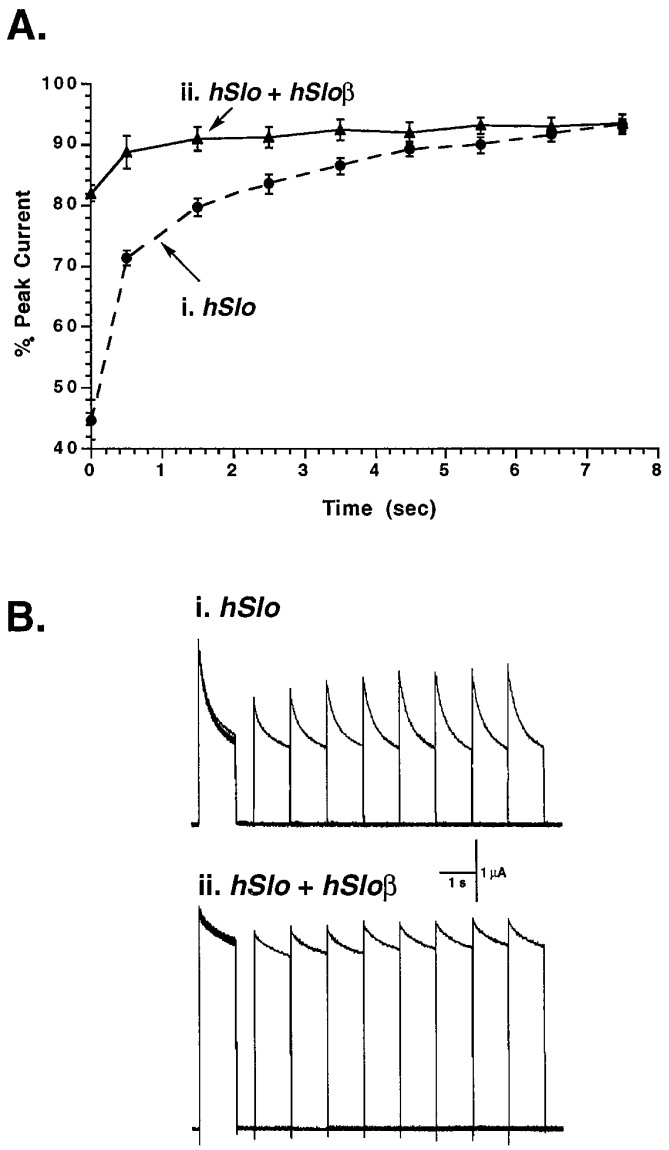

Figure 3. Slow current inactivation reduction in oocytes expressing *hSlo* + *hSloβ* relative to those expressing *hSlo*. *A*, In a paired-pulse paradigm, to examine the rate of recovery from inactivation, a 1 sec voltage step (−60 mV hold to 100 mV) was used as the "conditioning" stimulus to produce a significant level of inactivation (time 0, end of the conditioning pulse), followed at an increasing interval by a single identical "test" voltage step. Initial inactivation was measured by comparing the early peak current of the conditioning voltage step with the residual current at the end of the first step. Peak current amplitudes of the subsequent step in each paired episode were used to measure recovery. The conditioning step produced significantly greater levels of inactivation of *hSlo* currents compared with expressing *hSlo* + *hSloβ* currents (*t* test; $p < 0.001$), and recovery was significantly slower (repeated measures ANOVA, $F = 15.9$, $p = 0.005$). Full recovery was not achieved by 7.5 sec after the conditioning pulse. With longer single voltage steps (10 sec), a significant increase in the time course of inactivation was observed (*hSlo* τ_1 = 309.7 ± 36.2 msec, $n = 5$; *hSlo* + *hSloβ* τ_1 = 702.0 ± 88.2 msec, $n = 5$; $p = 0.003$, two-tailed *t* test; τ_2 values not reported because of contamination by slowly activating native current). *B*, Examples of current inactivation and its recovery resulting from the paired-pulse paradigm (8 sweeps) in oocytes expressing *hSlo* or *hSlo* + *hSloβ*. The level of inactivation was independent of current amplitude (expression level) within the normal limits encountered in this study. There was no inactivation of native Ca^{2+}-activated Cl^- current, and currents represent IbTX-sensitive current components, after subtraction of residual currents in supramaximal IbTX.

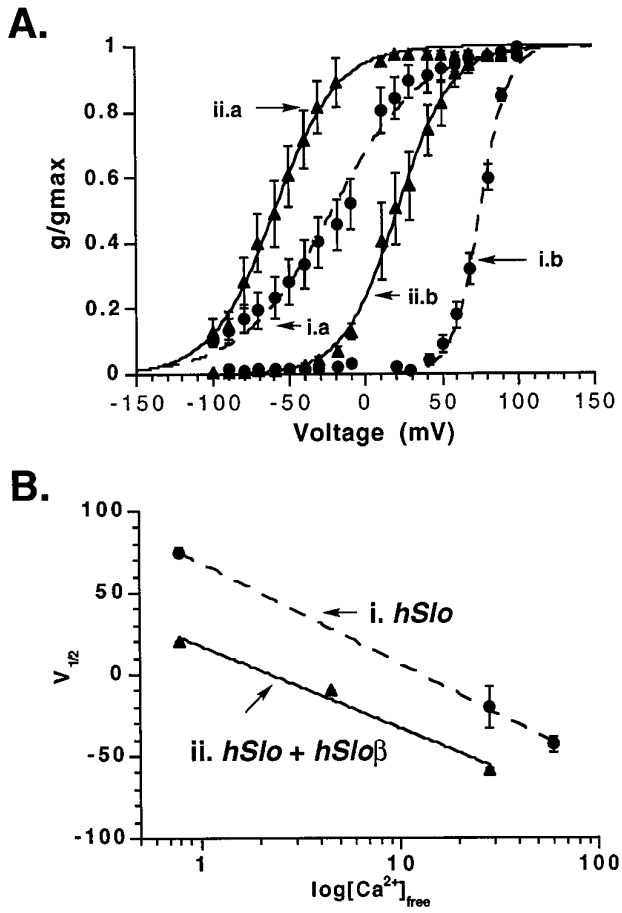

Figure 4. Coexpression of *hSlo* + *hSloβ* increased the sensitivity of BK channels to intracellular Ca^{2+}. *A*, Conductance (g/g_{max})/voltage (g/V) plots generated for *hSlo* (*i.*) and *hSlo* + *hSloβ* (*ii.*) in 28.2 μM Ca^{2+} (*a*) and 0.79 μM Ca^{2+} (*b*); recordings obtained from inside-out excised patches from transiently transfected HEK 293 cells in response to voltage ramps (−100 to 100 mV, 4 sec duration; data from a minimum of 25 ramps per patch). Note that at both concentrations of intracellular Ca^{2+}, the g/V relationship for *hSlo* + *hSloβ* is shifted to the left, indicating increased Ca^{2+} sensitivity. Curves were generated with a standard Boltzmann relationship in which $g/g_{max} = (1 + \exp[(V_{1/2} - V_m)/K])^{-1}$. *B*, The half-maximal activation values ($V_{1/2}$) for three concentrations of intracellular Ca^{2+} are plotted for *hSlo* and *hSlo* + *hSloβ*; $V_{1/2}$ values were consistently lower (as plotted) for *hSlo* coexpressed with the *hSloβ* subunit.

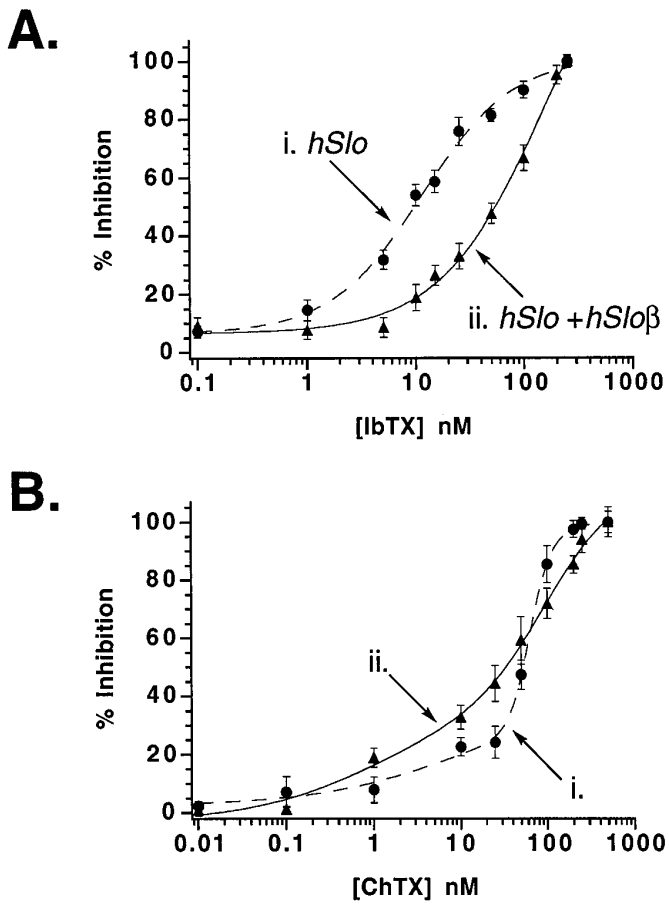

Figure 5. IBTX and ChTX pharmacology. *A*, Application of the BK channel-blocking peptide IbTX to oocytes expressing *hSlo* or *hSlo* + *hSloβ* revealed that coexpression with the *hSloβ* subunit resulted in a nearly 10-fold decrease in the sensitivity to IbTX blockade; n = 5–10 oocytes/IbTX concentration. Maximal effect was defined as the effect produced by incubation in 100–250 nM IbTX; maximal levels of suppression did not differ significantly between *hSlo* and *hSlo* + *hSloβ*. *B*, Application of the peptidyl blocker ChTX did not reveal a significantly different profile of blockade for *hSlo* and *hSlo* + *hSloβ*. Maximal effect was defined as the response to 250–500 nM ChTX, and maximal levels of effect did not differ between *hSlo* and *hSlo* + *hSloβ*.

voltage (g/V) relationship (Fig. 4*A*) and a reduction in the half-maximal activation voltage for any tested Ca^{2+} concentration (Fig. 4*B*).

Pharmacology of *hSlo*- and *hSlo* + *hSloβ*-mediated currents

To determine whether differences existed in the pharmacology of *hSlo*- and *hSlo* + *hSloβ*-mediated currents, we applied IbTX (Galvez et al., 1990; Giangiacomo et al., 1992) and ChTX (Miller et al., 1985; Sugg et al., 1990), which are high-affinity peptidyl blockers of the rat brain type I BK channel (Reinhart et al., 1989), and tetrandrine, an alkaloid blocker of the rat brain type II BK channel (Wang and Lemos, 1992), to oocytes and/or HEK 293 cells expressing these constructs. A marked difference in the sensitivity of the currents to both IbTX and tetrandrine was observed. The currents in oocytes expressing *hSlo* were significantly more sensitive to IbTX than those in oocytes expressing *hSlo* + *hSloβ* (Fig. 5*A*; EC_{50} = 11.4 nM for *hSlo*, EC_{50} = 163.7 for *hSlo* + *hSloβ*). Less effect of coexpression was observed in the responses to ChTX; a small increase in sensitivity was noted in the oocytes expressing *hSlo* + *hSloβ* (Fig. 5*B*), but these effects were not significant. The blockade by both peptides occurred more slowly in oocytes expressing *hSlo* + *hSloβ*, although this was not quantified. Application of the alkaloid tetrandrine to HEK 293 cells expressing either *hSlo* or *hSlo* + *hSloβ* revealed a concentration-dependent depression of BK current; however, the potency of blockade was much greater on *hSlo* + *hSloβ*-mediated currents (Fig. 6*A*). In addition, tetrandrine was shown to exacerbate the slower activation kinetics of the *hSlo* + *hSloβ* currents; this was particularly evident in the oocytes, in which tetrandrine produced a marked slowing of the current activation, with a significant increase in the latency to current peak (Fig. 6*B*). No consistent differences were observed in the concentration–response (1.0–100 μM) relationship of the benzimidazolone BK channel opener NS1619 (Olesen et al., 1994) between the two types of BK channels (Fig. 7). This was consistent with an earlier

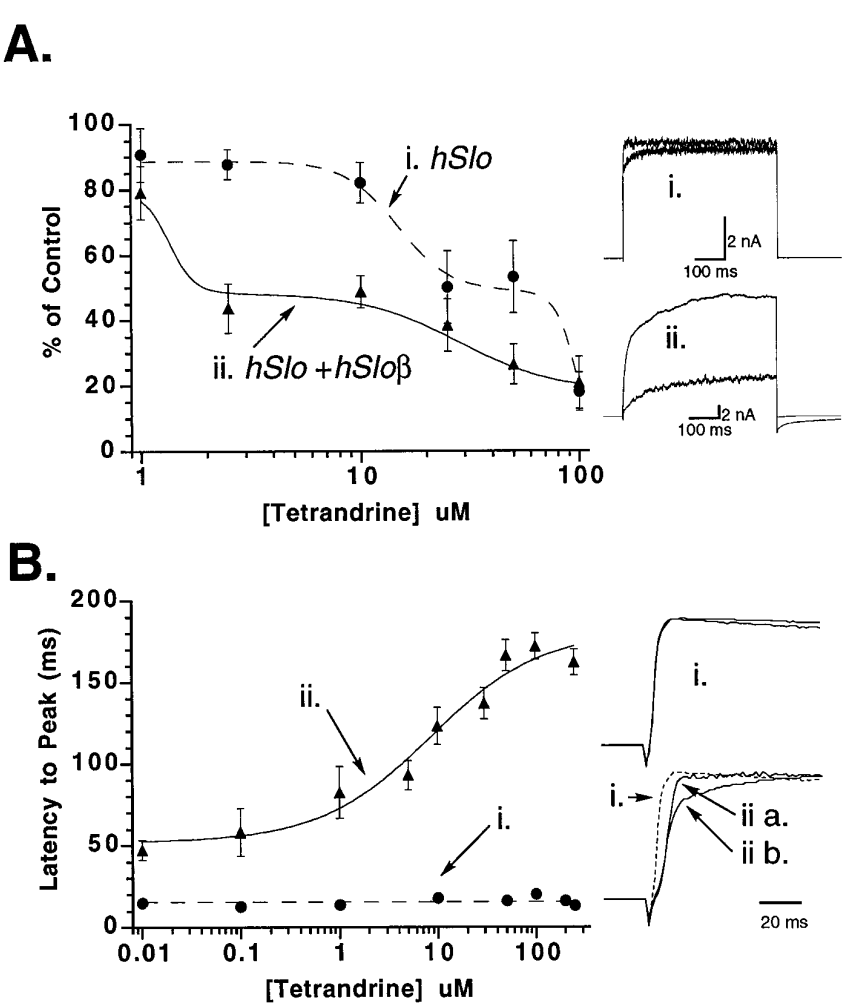

Figure 6. Tetrandrine pharmacology in oocytes and HEK 293 cells. *A*, Suppression of *hSlo*-mediated whole-cell membrane currents in HEK 293 cells by the alkaloid type II BK blocker tetrandrine was reduced relative to the degree of block observed in cells transfected with *hSlo* + *hSloβ*; n = 5–9 cells/tetrandrine concentration. The fitted curves suggest multiple affinity interactions of tetrandrine with both constructs; absolute maximal levels of tetrandrine block could not be determined because of limited solubility. The *traces* are examples of the relative effects of 2.5 μM tetrandrine on whole-cell HEK 293 BK membrane currents. Note that tetrandrine slowed activation of both types of current, but this effect was most pronounced with a greater level of block produced in cells expressing *hSlo* + *hSloβ*. *B*, A pronounced increase in the latency to current peak was observed only in oocytes expressing *hSlo* and *hSlo* + *hSloβ* when exposed to tetrandrine. *Traces* depict the effect of 50 μM tetrandrine (*b.*) on BK currents in oocytes expressing *hSlo* (*top traces; i.*), or *hSlo* + *hSloβ* (*bottom traces; ii.*), relative to control values (*a.*). The *dotted trace* in the *bottom set* is the control *hSlo* trace for comparison. Tetrandrine had no effect on the current activation in the *hSlo* oocyte, but it significantly delayed the peak of the current in the oocyte expressing *hSlo* + *hSloβ* (EC_{50} = 8.5 μM). The currents are the response to voltage steps from a holding potential of −60 to 100 mV, and only the initial portions of the normalized currents are depicted.

report that openers of this class, unlike DHS-1, did not distinguish between types of native BK channels (McKay et al., 1994).

Modulation of *hSlo*- and *hSlo* + *hSloβ*-mediated currents by PKA

BK channels are modulated by cAMP-dependent protein phosphorylation and dephosphorylation, with most type I channels increasing P_{open} in response to phosphorylation and most type II channels showing decreased activity when phosphorylated (Reinhart et al., 1989, 1991). The catalytic subunit of PKA was applied to the cytosolic side of *hSlo* and *hSlo* + *hSloβ* channels in excised membrane patches from transfected HEK 293 cells. The *hSlo* channels (6 of 6) showed a marked and reversible increase in P_{open} after exposure to PKA, whereas the majority of *hSlo* + *hSloβ* channels (5 of 8) showed a reduction in P_{open} (Fig. 8).

DISCUSSION

The slower activation of *hSlo* + *hSloβ* currents is unlikely to result from the increased Ca^{2+} sensitivity of these channels in the presence of the *hSloβ* subunit. A recent report (DiChiara and Reinhart, 1995) showed that increasing Ca^{2+} concentrations produced more rapid activation of *dSlo* and *hSlo* BK channels; assuming that increased Ca^{2+} sensitivity of *hSlo* in the presence of the *hSloβ* subunit acted like an apparent increase in Ca^{2+} concentration relative to *hSlo* channels when all other variables were equivalent, a decrease in activation time would be expected, rather than the observed increase. Increasing the step voltage likewise was shown to reduce activation time for *hSlo* (DiChiara and Reinhart, 1995). Although this was observed for both constructs, the significant difference in activation time and time to peak current was independent of the step voltage. The increased time to deactivation of *hSlo* + *hSloβ*, however, was consistent with an increase in Ca^{2+} sensitivity in the presence of the subunit (DiChiara and Reinhart, 1995), and we therefore cannot eliminate this as the cause of the slower deactivation/relaxation.

In some important respects, coexpression produced BK channels and currents consistent with Type II BK channel characteristics, whereas *hSlo* channels had some characteristics consistent with a Type I classification. The *hSlo* channels had greater sensitivity to IbTX, faster activation kinetics, and channel activity was upregulated by PKA, which are type I characteristics. The *hSlo* + *hSloβ* channels, on the other hand, were less sensitive to IbTX, had much slower activation kinetics, and were downregulated by PKA application, which are type II characteristics (Reinhart et al., 1989, 1991). The relatively greater effect of tetrandrine on *hSlo* + *hSloβ* currents was also phenotypically similar to type II BK channels. In a previous study, coexpression of a bovine β subunit (*bSloβ*) and a mouse *Slo* homolog (*mSlo*) resulted in an increase in Ca^{2+} sensitivity (McManus et al., 1995), which we likewise observed with coexpression of *hSlo* and *hSloβ*. Although they reported that coexpression resulted in the disappearance of brief closed events, they did not report detailed changes in channel

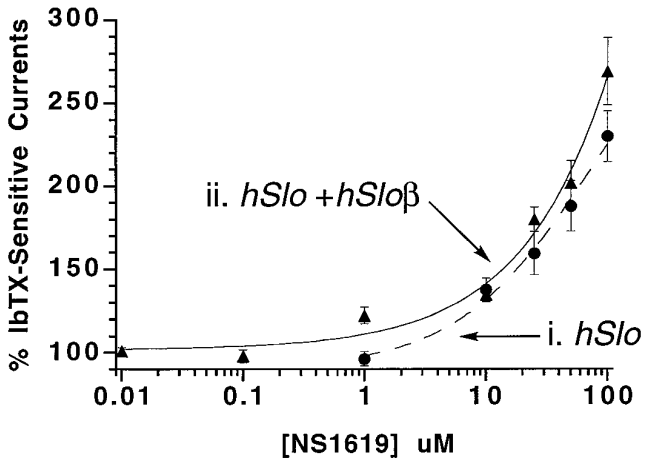

Figure 7. Effects of the application of the BK channel opener NS1619. At a range of NS1619 concentrations, oocytes injected with either *hSlo* or *hSlo* + *hSloβ* cRNA showed similar levels of activation of whole-cell BK currents. Measured currents represent the response to a voltage step from −60 to 140 mV. A minimum of five oocytes were used for each concentration of NS1619.

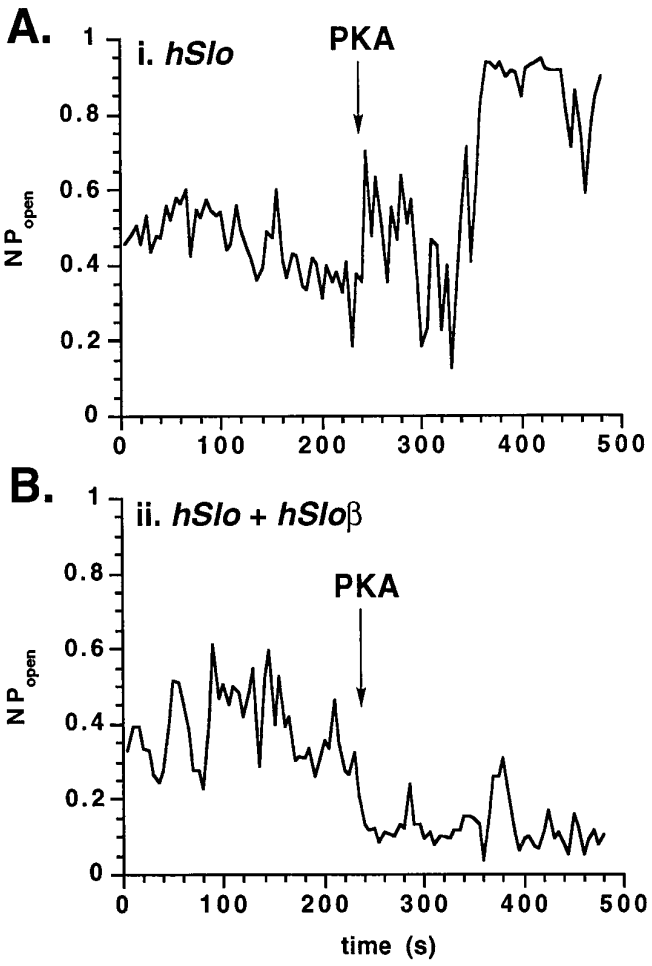

Figure 8. Modulation of *hSlo* and *hSlo* + *hSloβ* channels by exposure to PKA. *A*, Application of the catalytic subunit of PKA produced an increase in NP_{open} when applied to the cytosolic side of an inside-out membrane patch excised from an HEK 293 cell transiently expressing *hSlo*. *B*, PKA reduced NP_{open} in a patch excised from an HEK 293 cell transiently coexpressing *hSlo* + *hSloβ*. The mean increase in NP_{open} (averaged over the entire 240 sec control period vs the 240 sec PKA application) for *hSlo* patches was 97.1 ± 35.9% (SEM all) above control values ($n = 6$; increases seen in all 6 patches); the mean decrease in NP_{open} recorded from *hSlo* + *hSloβ* patches was −19.0 ± 15.6% ($n = 8$; 5 decreased, 1 no change, 2 increased, all data included in average; the difference was significant, $p < 0.03$, two-tailed t test). Partial recovery after removal of PKA was observed in some patches during a 240 sec wash period (data not shown).

kinetics or differences in sensitivity to toxin blockade. This may be the result of the constructs expressed; although mammalian *Slo* proteins are highly homologous (e.g., *mSlo* vs *hSlo*, 98% sequence identity; Dworetzky et al., 1994), it seems that *Sloβ* subunit sequences do not have the same degree of identity (Fig. 1), and these differences may be sufficient to affect expression and/or function. In at least two characteristics, however, we found variance with the original characterization of type I and type II channels. Type I channels were found to be somewhat more sensitive to $[Ca^{2+}]_{in}$ (Reinhart et al., 1989), which would be inconsistent with *hSlo* being the type I BK channel, based on our data and that of the previous study. In addition, the similar levels of block by ChTX suggests that this classification is not applicable to all of the BK channel phenotypic alterations produced by *Sloβ* subunit coexpression. However, we must also keep in mind that the original classification resulted from the characterization of rat brain BK channels, and differences with the human (*hSlo*) phenotype could underlie the observed variance.

Although we observed protein expression of *hSlo* and *hSloβ* separately in HEK 293 cells (data not shown), we have not demonstrated coexpression of both proteins within the same cell independent of electrophysiological recordings. Therefore, we could not eliminate recordings in which coexpression did not seem to be successful. This had the result of making the effects of coexpression seem more variable (note increased SEM values for most measures in cells expressing *hSlo* + *hSloβ*) and may have been a particular problem in the PKA experiments, in which the consequence of coexpression was a change in direction of modulation rather than in degree of effect. Nevertheless, these results indicate that in some important characteristics *hSlo* resembled the rat brain type I BK channel, whereas coexpression of the *hSloβ* subunit altered some characteristics of the expressed *hSlo* channel phenotype to a type II profile.

It was difficult to directly compare the quantitative measurements of our cloned expressed BK channels with those reported for native type I and type II BK channels. In particular, relatively few studies have focused on native populations of type I and type II BK channels, and experiments in these cases were generally performed in different systems and under different experimental conditions. Nevertheless, in the PKA experiments, we observed close to a doubling of P_{open} when *hSlo* channels were exposed to PKA, which is very similar to the values reported for the type I channel recorded from lipid bilayers (Reinhart et al., 1991). In the *hSlo* + *hSloβ* experiments, when PKA was applied to these channels, a small but significant decrease in P_{open} was observed that was not as large as the downregulation for the type II channels recorded in lipid bilayers. However, given that two of the patch recordings showed an increase after exposure to PKA, the results suggest the presence of a mixed population of channels, at least with respect to their response to phosphorylation, which may reflect the presence of both *hSlo* channels with and without coexpression of *hSloβ* despite cotransfection. If the channels in

which PKA did not produce an upregulation of P_{open} are considered alone, the PKA-induced decrease in P_{open} in patches from *hSlo* + *hSloβ*-transfected cells would then closely resemble the comparable reduction for native type II channels (Reinhart et al., 1991). In addition, estimated EC_{50} values for *hSlo*-expressing cells for BK channel blockers are within an order of magnitude of values similarly obtained for native (toxin-sensitive and presumably type I) BK channels (Reinhart et al., 1989; Giangiacomo et al., 1992). However, the *hSlo* + *hSloβ* toxin curves in Figures 5 and 6 seem to be shallow compared with *hSlo* alone and do not reflect the degree of insensitivity expected of a pure population of type II BK channels. The shallow curves may suggest the presence of two binding sites, again suggestive of a mixed population of channels, at least in the oocytes. Regardless of the exact degree or correspondence between cloned *hSlo* and *hSlo* + *hSloβ* BK channels and any previously described BK channel classification scheme, it is clear from the data presented in this study that the association of the BK-specific *hSloβ* subunit confers significant phenotypic alteration to *hSlo* channels. Thus, the *hSloβ* subunit is a likely major source of observed phenotypic variation in native BK channel populations, but is not the only source of BK channel diversity.

In conclusion, the changes in phenotype produced by this single known *Sloβ* subunit are significant and are manifest in several modalities. When coupled with changes produced by alternative splice variation, the contribution of the *hSloβ* subunit forms part of the molecular basis for native BK channel diversity. A better understanding of the interactions of these channels and their regulatory subunit(s) should provide insight into the structural determinants of BK channel modulation and its functional consequences on cellular physiology.

Note added in proof: Subsequent to the submission of this manuscript, Meera et al. (1996) report that coexpression of *hSlo* and *hSloβ* produced an increase in current activation time constants and an increase in Ca^{2+} sensitivity.

REFERENCES

Adelman JP, Shen K-Z, Kavanaugh MP, Warren RA, Wu Y-N, Lagrutta A, Bond CT, North RA (1992) Calcium-activated potassium channels expressed from cloned complementary DNAs. Neuron 9:206–216.

Atkinson NS, Robertson GA, Ganetzky B (1991) A component of calcium-activated potassium channels encoded by the *Drosophila slo* locus. Science 253:551–553.

Bielefeldt K, Jackson M (1993) A calcium-activated potassium channel causes frequency-dependent action-potential failures in a mammalian nerve terminal. J Neurophysiol 70:284–298.

Butler A, Tsunoda S, McCobb DP, Wei A, Salkoff L (1993) *mSlo*, a complex mouse gene encoding "maxi" calcium-activated potassium channels. Science 261:221–224.

Chandy KG, Gutman GA (1995) Voltage-gated potassium channel genes. In: Handbook of receptors and channels: ligand- and voltage-gated ion channels (North RA, ed), pp 1–71. Boca Raton, FL: CRC.

Colman A (1984) Translation of eukaryotic messenger RNA in *Xenopus* oocytes. In: Transcription and translation: a practical approach. (Hames BD, Higgins SJ, eds), pp 271–293. Oxford: IRC.

DiChiara TJ, Reinhart PH (1995) Distinct effects of Ca^{2+} and voltage on the activation and deactivation of cloned Ca^{2+}-activated K^+ channels. J Physiol (Lond) 489:403–418.

Dworetzky SI, Trojnacki JT, Gribkoff VK (1994) Cloning and expression of a human large-conductance calcium-activated potassium channel. Mol Brain Res 27:189–193.

Galvez A, Giminez-Gallago G, Reuben JP, Roy-Constancin L, Feigenbaum P, Kaczorowski GJ, Garcia ML (1990) Purification and characterization of a unique, potent, peptidyl probe for the high conductance calcium-activated potassium channel from venom of the scorpion *Buthus tamulus*. J Biol Chem 265:11083–11090.

Giangiacomo KM, Garcia ML, McManus OB (1992) Mechanism of iberiotoxin block of the large-conductance calcium-activated potassium channel from bovine aortic smooth muscle. Biochemistry 31:6719–6727.

Hamill OP, Marty O, Neher E, Sakman B, Sigworth FJ (1981) Improved patch-clamp techniques for high-resolution current recordings from cells and cell-free membrane patches. Pflügers Arch 391:85–100.

Knaus H-G, Folander K, Garcia-Calvo M, Garcia ML, Kaczorowski G, Smith M, Swanson R (1994) Primary sequence and immunological characterization of β-subunit of high conductance Ca^{2+}-activated K^+ channel from smooth muscle. J Biol Chem 269:17274–17278.

Kozak M (1987) An analysis of 5′-noncoding sequences from 699 vertebrate messenger RNAs. Nucleic Acids Res 15:8125–8148.

Lagrutta A, Shen K-Z, North RA, Adelman JP (1994) Functional differences among alternatively spliced variants of *slowpoke*, a *Drosophila* calcium-activated potassium channel. J Biol Chem 269:20347–20351.

Latorre R, Oberhauser A, Labarca P, Alvarez O (1989) Varieties of calcium-activated potassium channels. Annu Rev Physiol 51:385–399.

McCobb DP, Fowler NL, Featherstone T, Lingle CJ, Saito M, Krause JE, Salkoff L (1995) Am J Physiol 38:H767–H777.

McKay MC, Dworetzky SI, Meanwell NA, Olesen S-P, Reinhart PH, Levitan IB, Adelman JP, Gribkoff VK (1994) Opening of large-conductance calcium-activated potassium channels by the substituted benzimidazolone NS004. J Neurophysiol 71:1873–1882.

McManus OB, Helms LMH, Pallanck L, Ganetzky B, Swanson R, Leonard RJ (1995) Functional role of the β subunit of high conductance calcium-activated potassium channels. Neuron 14:645–650.

Meera P, Wallner M, Jiang Z, Toro L (1996) A calcium switch for the functional coupling between α (*hSlo*) and β subunits (K_V, $_{Ca}\beta$) of maxi K channels. FEBS Lett 382:84–88.

Miller C, Moczydlowski E, Latorre R, Phillips M (1985) Charybdotoxin, a protein inhibitor of single Ca^{2+}-activated K^+ channels from mammalian skeletal muscle. Nature 313:316–318.

Olesen S-P, Munch E, Moldt P, Drejer J (1994) Selective activation of Ca^{2+}-dependent K^+ channels by novel benzimidazolone. Eur J Pharmacol 251:53–57.

Pallanck L, Ganetzky B (1994) Cloning and characterization of human and mouse homologs of the *Drosophila* calcium-activated potassium channel gene, slowpoke. Hum Mol Genet 3:1239–1243.

Pongs O (1992) Molecular biology of voltage-dependent potassium channels. Physiol Rev [Suppl] 72:S69–S88.

Reinhart PH, Chung S, Levitan IB (1989) A family of calcium-dependent potassium channels from rat brain. Neuron 2:1031–1041.

Reinhart PH, Chung S, Martin BL, Brautigan DL, Levitan IB (1991) Modulation of calcium-activated potassium channels from rat brain by protein kinase A and phosphatase 2A. J Neurosci 11:1627–1635.

Rettig J, Heinemann SH, Wunder F, Lorra C, Parcej DN, Dolly JO, Pongs O (1994) Inactivation properties of voltage-gated K^+ channels altered by presence of β-subunit. Nature 369:289–294.

Robitaille R, Charlton MP (1992) Presynaptic calcium signals and transmitter release are modulated by calcium-activated potassium channels. J Neurosci 21:297–303.

Salkoff L, Baker K, Butler A, Covarrubias M, Pak MD, Wei A (1992) An essential "set" of K^+ channels conserved in flies, mice, and humans. Trends Neurosci 15:161–166.

Stuhmer W (1992) Electrophysiology recording from *Xenopus* oocytes. In: Methods in enzymology: ion channels, Vol 207 (Rudy B, Iverson LE, eds), pp 319–339. San Diego, CA: Academic.

Sugg EE, Garcia ML, Reuben JP, Patchett AA, Kaczorowski G (1990) Synthesis and structural characterization of charybdotoxin, a potent peptidyl inhibitor of the high-conductance Ca^{2+}-activated K^+ channel. J Biol Chem 265:18745–18748.

Tseng-Crank J, Foster CD, Krause JD, Mertz R, Godinot N, DeChiara TJ, Reinhart PH (1994) Cloning, expression, and distribution of functionally distinct Ca^{2+}-activated K^+ channel isoforms from human brain. Neuron 13:1315–1330.

Wang G, Lemos JR (1992) Tetrandrine blocks a slow, large-conductance Ca^{2+}-activated potassium channel besides inhibiting a non-inactivating Ca^{2+} current in isolated terminal of the rat neurohypophysis. Pflügers Arch 421:558–565.